Supporting Information

Direct Plasmon-Enhanced Electrochemistry for Enabling Ultrasensitive and Label-Free Detection of Circulating Tumor Cells in Blood

Shan-Shan Wang,[†] Xiao-Ping Zhao,[†] Fei-Fei Liu,[†] Muhammad Rizwan Younis,[‡] Xing-Hua Xia,[*‡] Chen Wang[*†]

[†]Key Laboratory of Drug Quality Control and Pharmacovigilance, Ministry of Education; Key Laboratory of Biomedical Functional Materials, School of Science, China Pharmaceutical University, Nanjing, 211198, China

[‡]State Key Laboratory of Analytical Chemistry for Life Science, School of Chemistry and Chemical Engineering, Nanjing University, Nanjing 210093, China

*To whom correspondence should be addressed. E-mail: xhxia@nju.edu.cn; wangchen@cpu.edu.cn

Supporting Information Table of Contents

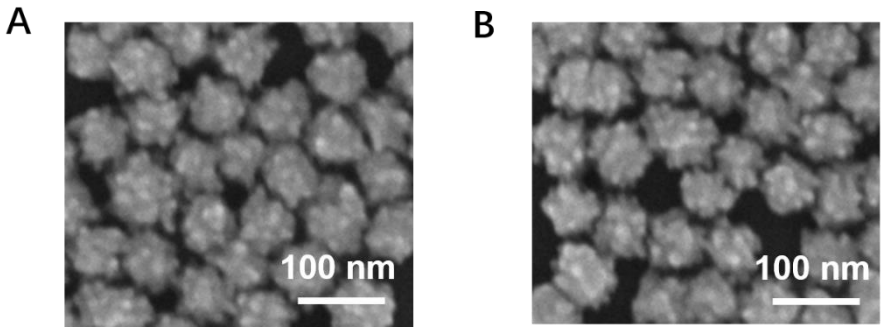

Figure S1. SEM images of the AuNSs deposited on GC substrate before (A) and after (B) experiment.

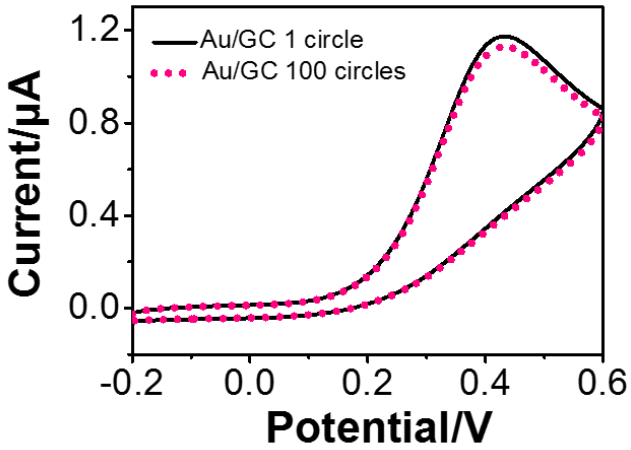

Figure S2. CV curves of the AuNSs/GC electrode in the presence of 1 mM AA at 1st circle and 100th circle.

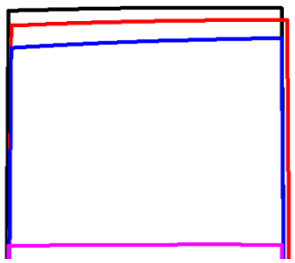

Figure S3. The magnification of I-t curves of Figure 2B.

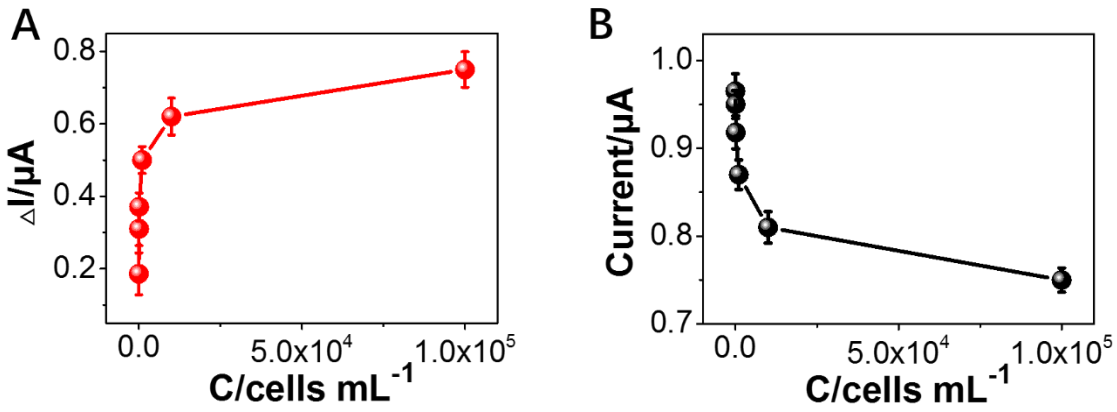

Figure S4. (A) The changed current value versus the concentrations of CCRF-CEM cells ranging from 5 to 1×10^5 cells/mL. (B) The peak current values in Figure 5C versus the concentrations of CCRF-CEM cells ranging from 5 to 1×10^5 cells/mL.

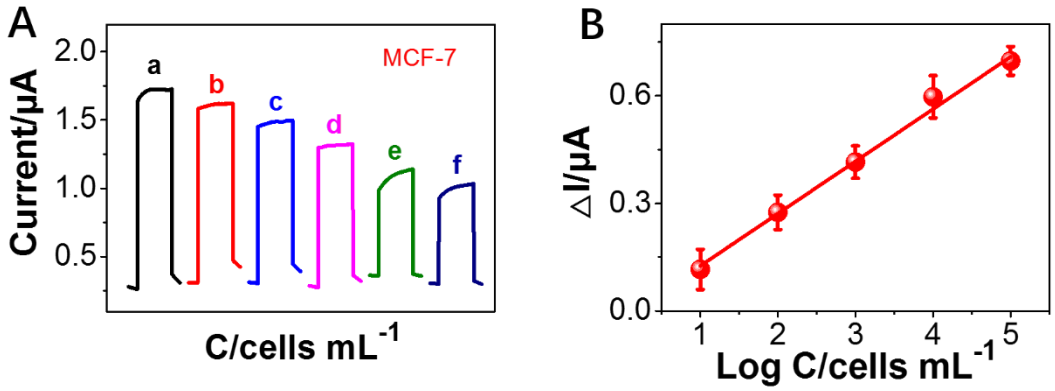

Figure S5. (A) *I*−*t* curves of the electrode after capturing different concentrations of MCF-7 cells with light on and off. The concentration of curve (a-f) is 0, 10, 1×10^2, 1×10^3, 1×10^4, 1×10^5 cells/mL respectively. (B) The linear relationship between the current change (ΔI) and the logarithm value of cells concentration in the range from 10 to 1×10^5 cells/mL.

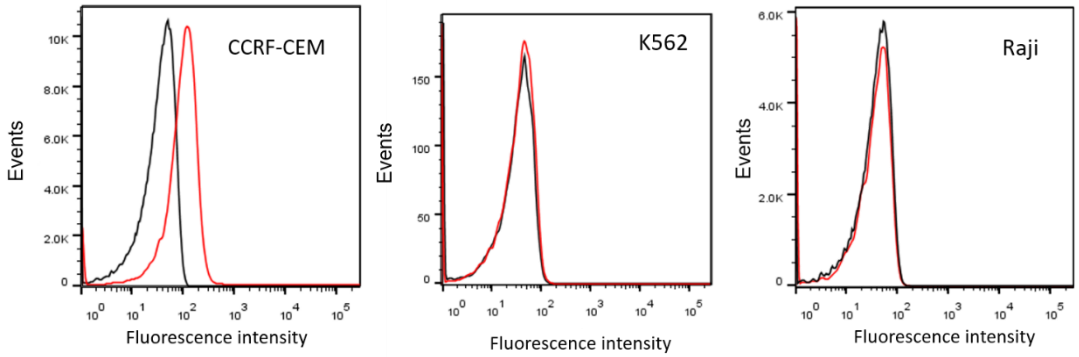

Figure S6. Flow cytometry analysis of CCRF-CEM, K562, Raji cells (Black curves, cells before incubation with FAM-sgc8c; Red curves, cells after incubation with FAM-sgc8c).

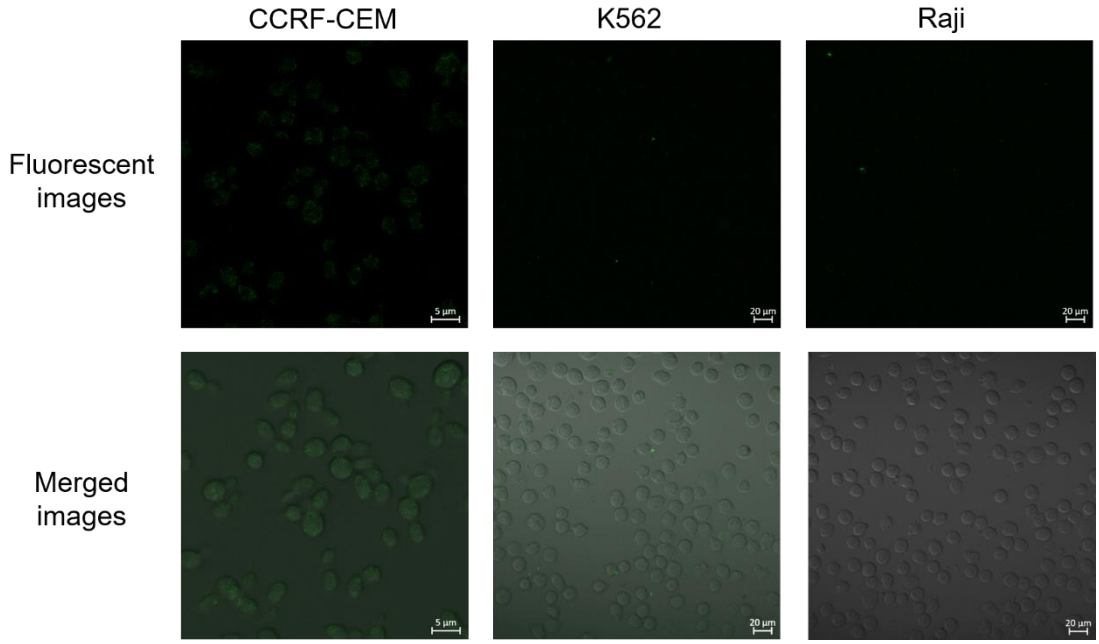

Figure S7. Confocal microscopy images of CCRF-CEM, K562, Raji cells incubated with FAM-Sgc8c.

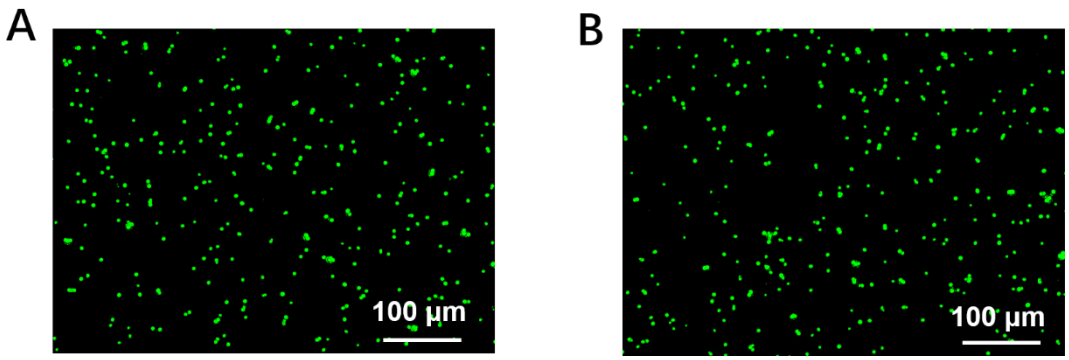

Figure S8. Fluorescence microscope images of CCRF-CEM cells after and before 808 nm laser irradiation (200 mW).

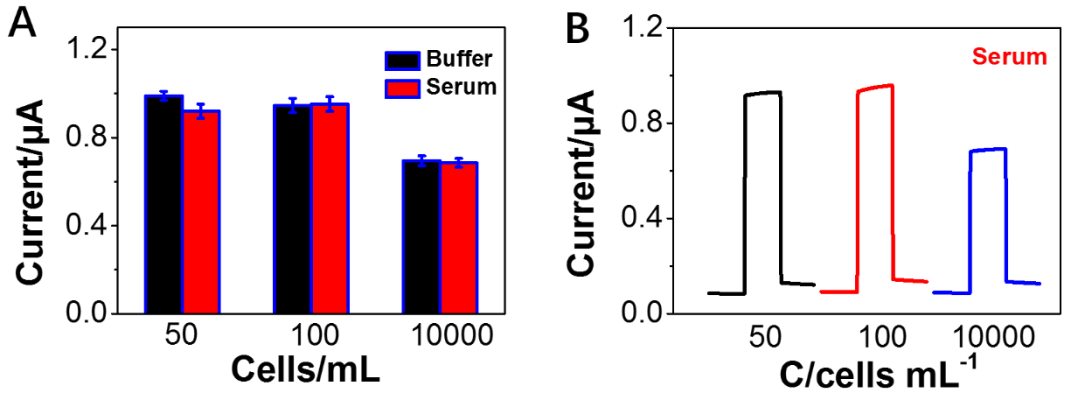

Figure S9. (A) The detection CTCs in different samples. Results were obtained from the PBS buffer solution and diluted human serum samples. (B) *I-t* curves of the aptamer/AuNSs/GC electrode incubation with different concentrations of CCRF-CEM cells in serum with light on and off.

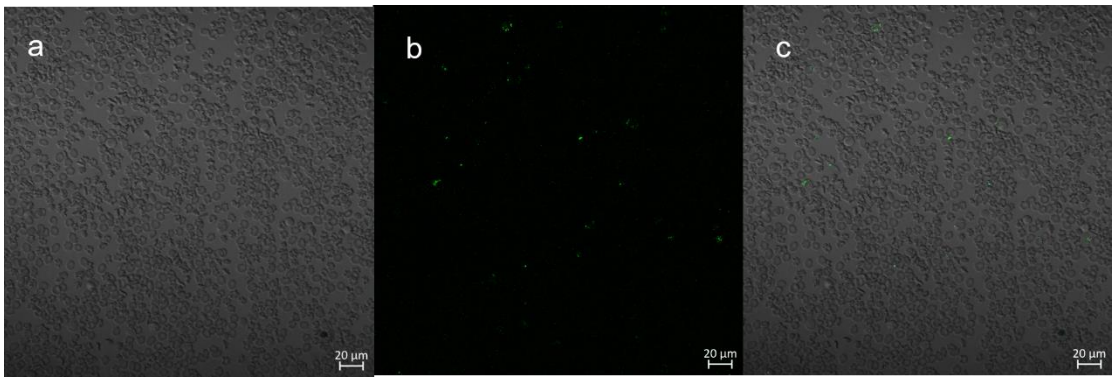

Figure S10. Confocal microscopy images of blood cells incubated with FAM-Sgc8c (a, Bright-field image; b, Fluorescent image; c, Merged image)

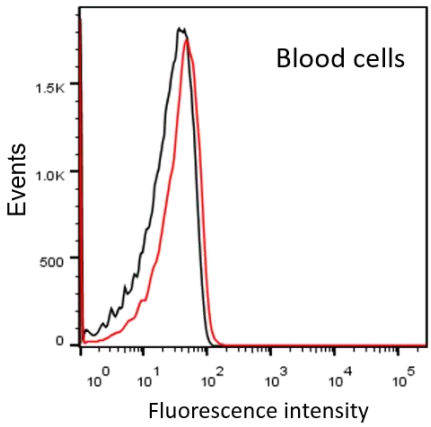

Figure S11. Flow cytometry analysis of blood cells. (Black curves, cells before incubation with FAM-sgc8c; Red curves, cells after incubation with FAM-sgc8c).

Table S1: Values of Rct for the Stepwise Construction of the Cytosensor

assembly process	Rct (Ω)
bare GCE	444.523
AuNSs	402.190
Aptamer	520.683
MCH	587.951
CCRF-CEM cells	7117.912

Table S2: Comparison of Cytosensors Performance for CCRF-CEM

Cytosensor	Detection method	Linear range	Detection limit	Reference
aptamer/GO	Fluorescence	1×10^2-1×10^7	100	S1
aptamer/GMNPs	DPV	10-1×10^6	10	S2
aptamer/ZnO NDs@g-C3N4 QDs	I-t	20-2×10^4	20	S3
aptamer-PCR	Fluorescence	100-2×10^3	100	S4
aptamer/PAA	LSV	100-1×10^6	100	S5
aptamer- microfluidic	Fluorescence	25-2.5×10^4	25	S6
aptamer/Ag NCs	Flow cytometry	7.5×10^3-6.25×10^5	7500	S7
HA-MNPs	QCM	8×10^3-1×10^5	8000	S8
aptamer/APBA-MWCNTs	EIS	1×10^3-1×10^7	1000	S9
aptamer/AuNSs	I-t	5-1×10^5	5	this work

Notes: GO: graphene oxide; GMNPs: gold nanoparticles-coated magnetic Fe_3O_4

nanoparticles; ZnO NDs@g-C_3N_4 QDs: ZnO nanodisks@g-C_3N_4 quantum dots; PCR: polymerase chain reaction; PAA: porous anodic alumina; Ag NCs: silver nanoclusters; HA-MNPs: hyaluronic acid-coated magnetic nanoparticles; APBA-MWCNTs: 3-aminophenylboronic acid-functionalized multiwalled carbon nanotubes; DPV: differential pulse voltammetry; LSV: linear sweep voltammetry；QCM, quartz crystal microbalance; EIS: electrochemical impedance spectroscopy.

Table S3: Determination of CCRF-CEM Cells in Human Blood (n=5) with the Cytosensors.

Spiked cells (cells mL^{-1})	Detected cells (cells mL^{-1})	Recovery (%)	RSD (%)
50	58	116.00	6.88
100	106	106.00	5.33
1000	933	93.30	4.34
10000	9268	92.68	3.68

REFERENCE

(S1) Tan, J.; Lai, Z.; Zhong, L.; Zhang, Z.; Zheng, R.; Su, J.; Huang, Y.; Huang, P.; Song, H.; Yang, N.; Zhou, S.; Zhao, Y. A Graphene Oxide-Based Fluorescent Aptasensor for the Turn-on Detection of CCRF-CEM. *Nanoscale Res. Lett.* **2018**, *13*, 66.

(S2) Khoshfetrat, S. M.; Mehrgardi, M. A. Amplified detection of leukemia cancer cells using an aptamer-conjugated gold-coated magnetic nanoparticles on a nitrogen-doped graphene modified electrode. *Bioelectrochemistry* **2017**, *114*, 24-32.

(S3) Pang, X. H.; Cui, C.; Su, M. H.; Wang, Y. G.; Wei, Q.; Tan, W. H. Construction

of self-powered cytosensing device based on ZnO nanodisks@ g-C3N4 quantum dots and application in the detection of CCRF-CEM cells. *Nano energy* **2018**, *46*, 101-109.

(S4) Tang, J. L.; He, X. X.; Lei, Y. L.; Shi, H.; Guo, Q. P; Liu, J. B; He, D.; Yan, L.; Wang, K. Temperature-responsive split aptamers coupled with polymerase chain reaction for label-free and sensitive detection of cancer cells. *Chem. Commun.* **2017**, *53*, 11889-11892.

(S5)Cao, J.; Zhao, X. P.; Younis, M. R.; Li, Z. Q.; Xia, X. H.; Wang, C. Ultrasensitive Capture, Detection, and Release of Circulating Tumor Cells Using a Nanochannel-Ion Channel Hybrid Coupled with Electrochemical Detection Technique. *Anal. Chem.* **2017**, *89*, 10957-10964.

(S6) Cao, L. L; Cheng, L. W.; Zhang, Z. Y.; Wang, Y.; Zhang, X. X.; Chen, H.; Liu, B. H.; Zhang, S.; Kong, J. L. Visual and high-throughput detection of cancer cells using a graphene oxide-based FRET aptasensing microfluidic chip. *Lab. Chip.* **2012**, *12*, 4864-4869.

(S7) Yin, J.; He, X.; Wang, K.; Xu, F.; Shangguan, J.; He, D.; Shi, H. Label-Free and Turn-on Aptamer Strategy for Cancer Cells Detection Based on a DNA–Silver Nanocluster Fluorescence upon Recognition-Induced Hybridization. *Anal. Chem.* **2013**, *85*, 12011-12019.

(S8) Zhou, Y.; Xie, Q. Hyaluronic acid-coated magnetic nanoparticles-based selective collection and detection of leukemia cells with quartz crystal microbalance. *Sens. Actuators, B* **2016**, *223*, 9-14.

(S9) Paredes-Aguilera, R.; Romero-Guzman, L.; Lopez-Santiago, N.; Burbano-Ceron, L.; Camacho-Del Monte, O.; Nieto-Martinez, S. Flow cytometric analysis of cell‐surface and intracellular antigens in the diagnosis of acute leukemia. *Am. J. Hematol.* **2001**, *68*, 69-74.